

# PCCP

Accepted Manuscript



This is an *Accepted Manuscript*, which has been through the Royal Society of Chemistry peer review process and has been accepted for publication.

*Accepted Manuscripts* are published online shortly after acceptance, before technical editing, formatting and proof reading. Using this free service, authors can make their results available to the community, in citable form, before we publish the edited article. We will replace this *Accepted Manuscript* with the edited and formatted *Advance Article* as soon as it is available.

You can find more information about *Accepted Manuscripts* in the [Information for Authors](#).

Please note that technical editing may introduce minor changes to the text and/or graphics, which may alter content. The journal's standard [Terms & Conditions](#) and the [Ethical guidelines](#) still apply. In no event shall the Royal Society of Chemistry be held responsible for any errors or omissions in this *Accepted Manuscript* or any consequences arising from the use of any information it contains.



Cite this: DOI: 10.1039/xxxxxxxxxx

## A novel crystalline SiCO compound

Miriam Marqués,<sup>\*a</sup> Angel Morales-García,<sup>b</sup> José Manuel Menéndez,<sup>c</sup> Valentín G. Baonza<sup>b</sup> and José Manuel Recio<sup>c</sup>

Received Date  
Accepted Date

DOI: 10.1039/xxxxxxxxxx

www.rsc.org/journalname

*Ab initio* evolutionary structural searches have been performed on  $\text{Si}_x\text{C}_y\text{O}_{2(x+y)}$  compounds. A novel structure, with  $\text{SiC}_2\text{O}_6$  stoichiometry and  $P2_1/c$  space group is calculated to be stable against decomposition in a wide pressure window from 7.2 to 41 GPa, and metastable under ambient conditions. It consists of  $\text{CO}_3$  units, linked to  $\text{SiO}_6$  octahedra, supporting previous experimental studies. The evolution of the carbon environment towards tetrahedral  $\text{CO}_4$  units, thus resembling the crystal chemistry of silicon, is predicted at higher pressures.

### 1 Introduction

Understanding the processes involved in the complex global carbon cycle and its coupling to other elemental cycles (oxygen, nitrogen, iron, silicon...) remains a challenge. A vital step is unveiling the structure, bonding and phase stability of the carbon-bearing compounds in the Earth's mantle conditions<sup>1</sup>. On the other hand, the critical influence of atmospheric  $\text{CO}_2$  (main greenhouse gas) on Earth's climate and the increasing concern on global warming have led to a renewed interest on this area with the development of different  $\text{CO}_2$  sequestration techniques<sup>2</sup>. Nowadays, it is assumed that calcium and magnesium carbonates are the dominant oxidized carbon species in the mantle<sup>3</sup>. Most importantly,  $\text{CO}_2$  is produced through decarbonating reactions with silica in subducted basalts and released into the oceans and atmosphere during volcanic activity<sup>4,5</sup>. Therefore, the importance of the analysis of the  $\text{CO}_2$ - $\text{SiO}_2$  reactivity is clear.

Although  $\text{CO}_2$  and  $\text{SiO}_2$  do not react at ambient conditions, their structural analogies at high pressure raise the question whether any Si-C-O crystalline phase may exist. An interface consisting of unknown SiCO compounds has been in fact attributed to the oxidized silicon carbide<sup>6</sup> and previous *ab initio* studies proposed hypothetical  $\text{Si}_{(1-x)}\text{C}_x\text{O}_2$  structures generated by replacing silicon atoms by carbon atoms on the  $\alpha$ -quartz and the distorted- $\beta$ -cristobalite-like ( $I\bar{4}2d$ )  $\text{SiO}_2$  reference structures<sup>7,8</sup>. However, none of the generated structures was found to be thermodynamically stable. Also, recent experiments performed by Santoro *et al.* at 18-26 GPa and 600-980 K by reacting silicalite, a microporous

zeolite, and molecular  $\text{CO}_2$  filling the pores claimed the synthesis of a silicon carbonate phase with  $\text{CO}_3$  units<sup>9</sup>. Even more recently, at 16-22 GPa and temperatures in excess of 4000 K, the same authors have claimed the synthesis of a solid solution with an average chemical formula of  $\text{C}_{0.6}\text{Si}_{0.4}\text{O}_2$ <sup>10</sup>. X-ray diffraction showed that carbon and silicon atoms were randomly distributed in the cationic site of an  $\alpha$ -cristobalite-type structure. Therefore, both, carbon and silicon atoms were fourfold coordinated to oxygen atoms.

Interestingly, we had already proposed the  $\text{SiC}_2\text{O}_6$  ( $\approx \text{C}_{0.6}\text{Si}_{0.4}\text{O}_2$ ) stoichiometry as the most plausible one for silicon carbonate compounds based on stability studies on the  $\text{UB}_2\text{O}_6$ -type structure<sup>11</sup>. Subsequent structural searches with the Universal Structure Predictor: Evolutionary Xtallography (USPEX) code at 20 GPa confirmed the stability of the  $\text{SiC}_2\text{O}_6$  stoichiometry, with a  $P\bar{3}$  structure consisting of  $\text{SiO}_6$  and  $\text{CO}_3$  units as the lowest enthalpy structure<sup>12</sup>.

In this paper, we explore the existence of cationic-ordered crystalline systems containing just C, Si and O in a wide pressure range, from 0 GPa to 100 GPa. It opens the way for a new class of stable carbonate compounds at pressures close to the Earth's mantle conditions, with possible implications in the understanding of the deep carbon cycle and the carbon storage<sup>13,14</sup>.

### 2 Methods

We present here results from extensive structural searches of crystalline systems containing only these three elements within the general stoichiometric formula  $\text{Si}_x\text{C}_y\text{O}_{2(x+y)}$ , with  $x$  and  $y$  varying between 1 and 3, and up to 4 formula units in the simulation cell. These searches have been performed with the USPEX<sup>15</sup> code at selected pressures from 0 to 100 GPa. This code has successfully predicted the crystal structures of a large number of different systems, including carbonates<sup>16-18</sup>.

Each generation contains  $40 \times Z$  structures,  $Z$  being the number of formula units per cell, 60% of which are generated by heredity,

<sup>a</sup> MALTA-Consolider Team and Departamento de Física Teórica, Universidad de Valladolid, E-47011 Valladolid, Spain. Fax: +34983423013 ; Tel: +34983184571 ; E-mail: miriam.marques@uva.es

<sup>b</sup> MALTA-Consolider Team and Departamento de Química Física I, Universidad Complutense de Madrid, E-28040 Madrid, Spain.

<sup>c</sup> MALTA-Consolider Team and Departamento de Química Física y Analítica, Universidad de Oviedo, E-33006 Oviedo, Spain.

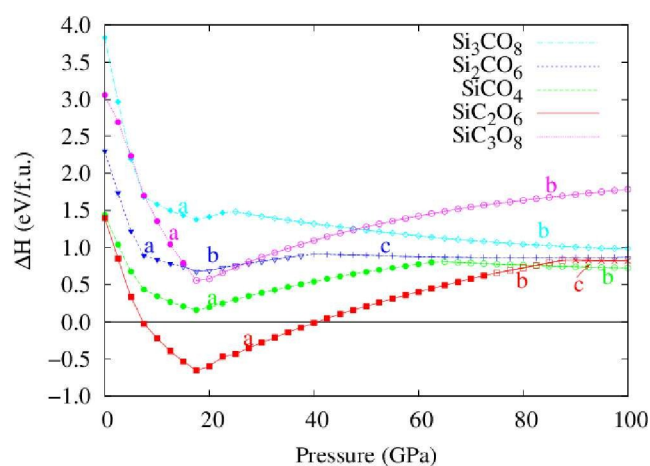


**Fig. 1** Calculated enthalpies of formation as a function of pressure for the lowest enthalpy structures corresponding to each stoichiometry. Both, cell parameters and internal coordinates were relaxed at each pressure. The enthalpy of the stable  $\text{SiO}_2$  and  $\text{CO}_2$  polymorphs at the corresponding pressure is taken as the reference enthalpy.  $\Delta H = H(\text{Si}_x\text{C}_y\text{O}_{(2x+2y)}) - xH(\text{SiO}_2) - yH(\text{CO}_2)$ . Different symbols and labels for each stoichiometry correspond to different structures. Specifically, the lowest enthalpy structures on increasing pressure have been labelled following the alphabetic order, a), b), (and c)).

and the others by random choice. We followed 30-60 generations (depending on the size of the system) to achieve the converged structure. Apart from randomly generated cationic-ordered crystalline structures, the initial search space of some of the searches also included structures derived from known  $\text{SiO}_2$  and  $\text{CO}_2$  polymorphs as well as others containing  $\text{CO}_4$ ,  $\text{SiO}_4$ ,  $\text{CO}_3$  and  $\text{SiO}_6$  units, potential constituents of the SiCO compounds. The underlying DFT *ab-initio* calculations were performed with the VASP code<sup>19</sup>. We used the Perdew-Burke-Ernzerhof generalized gradient (GGA) exchange-correlation functional<sup>20</sup> and the projector augmented wave (PAW) all-electron description of the electron-ion-core interaction<sup>21</sup>. Brillouin zone integrals were approximated using the method of Monkhorst and Pack<sup>22</sup>, and the energies converged with respect to  $k$ -point density ( $k$ -point grid spacing of  $2\pi \times 0.03 \text{ \AA}^{-1}$ ) and to the plane wave kinetic energy cutoff (600 eV). Phonons were calculated within density-functional perturbation theory<sup>23</sup> as implemented in the QUANTUM-ESPRESSO code<sup>24</sup>.

## 3 Results and discussion

### 3.1 Phase stability

The enthalpies of the formation reaction,  $x\text{SiO}_2 + y\text{CO}_2 \rightarrow \text{Si}_x\text{C}_y\text{O}_{(2x+2y)}$ , for the most stable phases of the different stoichiometries at their corresponding pressure stability ranges are plotted in Fig. 1. We have considered the structures for  $\text{SiO}_2$  and  $\text{CO}_2$  at 0 K in their corresponding stable pressure ranges, i.e.  $\text{SiO}_2$  in the  $\alpha$ -quartz (0 - 4.8 GPa), coesite (4.8 - 8.5 GPa), stishovite (8.5 - 55 GPa),  $\text{CaCl}_2$ -type (55 - 85 GPa) and  $\text{PbO}_2$ -type (85 - 100 GPa) structures and  $\text{CO}_2$  in the  $Pa\bar{3}$  (0 - 13 GPa),  $P4_2/mnm$  (13 - 18.2 GPa), and tetragonally-distorted  $\beta$ -cristobalite-like,  $I\bar{4}2d$  (18.2 - 100 GPa) structures. A maximum of two formula units

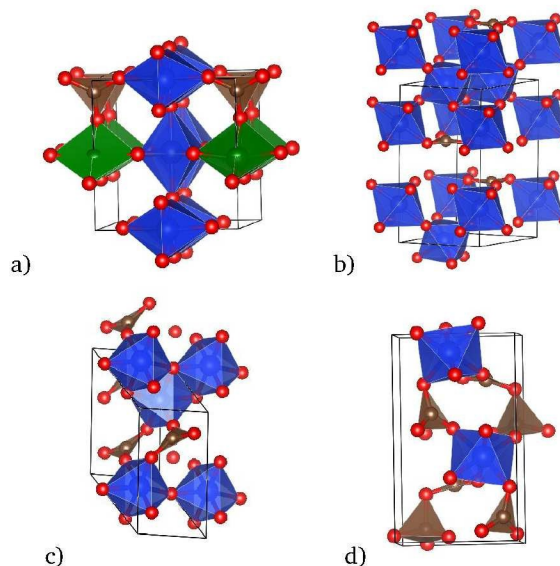


**Fig. 2** Unit cells of the lowest enthalpy polymorphs corresponding to the a)  $\text{Si}_3\text{CO}_8$ , b)  $\text{Si}_2\text{CO}_6$ , c)  $\text{SiCO}_4$ , and d)  $\text{SiC}_3\text{O}_8$  stoichiometries at the minima region. Coordination polyhedra for silicon and carbon atoms in blue and brown, respectively. In  $\text{Si}_3\text{CO}_8$ , coordination polyhedra for 5-coordinated silicon atoms in green.

per cell was enough to obtain the lowest enthalpy structures associated to each stoichiometry, with a number of generations between 30-50. The problem becomes much more complex when the number of formula units is four. It forced us to repeat simulations several times to achieve the same structures obtained when  $Z=2$ . At ambient conditions, none of the SiCO phases was found to be energetically stable versus decomposition. It agrees with the reported absence of reactivity between  $\text{SiO}_2$  and  $\text{CO}_2$  at those conditions. In fact, the structural searches at pressures below 5 GPa lead to structures with exceedingly big volume and molecular  $\text{CO}_2$  units, a signpost of the expected dissociation. Therefore, the graph only includes the lowest enthalpy structures for each stoichiometry found above 5 GPa. On pressure increase, the positive enthalpies of formation for all the stoichiometries decrease, presenting a minima region in the experimental range of stability of the previously synthesized SiCO phases.

### 3.2 $\text{Si}_3\text{CO}_8$ , $\text{Si}_2\text{CO}_6$ , $\text{SiCO}_4$ , and $\text{SiC}_3\text{O}_8$

Structurally, the lowest enthalpy structures in the minima enthalpic region consist of  $\text{SiO}_6$  and  $\text{CO}_3$  units, differing in the distortion, arrangement and the connectivity between them (see Fig. 2).

For instance, in  $\text{Si}_3\text{CO}_8$ ,  $2/3$  of the Si atoms (blue) form almost regular octahedra, whereas the coordination of the remaining Si atoms (green) is rectangular pyramidal (5-coordinated Si atoms). The almost planar  $\text{CO}_3$  units are corner-connected to the octahedra. There is also edge-sharing by the octahedra. For  $\text{Si}_2\text{CO}_6$ , the lowest enthalpy structure is laminar, with slabs consisting of two external layers of C atoms and 3 internal layers of Si atoms. The distribution of the O atoms on the layers of C atoms and between the Si layers generates an octahedral coordination for the



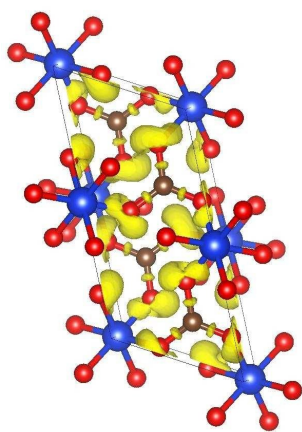


**Fig. 3**  $P2_1/c$  structure. Blue, brown and red spheres correspond to Si, C and O atoms. ELF isosurface (ELF=0.8) in yellow.

Si atoms and a triangular planar coordination for the C atoms. There is sharing of edges by octahedra. The  $\text{CO}_3$  units are corner-connected to  $\text{SiO}_6$  polyhedra. For  $\text{SiCO}_4$  each distorted  $\text{SiO}_6$  octahedron shares two edges with two adjacent  $\text{SiO}_6$  octahedra and is connected through three  $\text{CO}_3$  units to three extra octahedra. For  $\text{SiC}_3\text{O}_8$ , 1/3 of the C atoms adopt a strongly distorted tetrahedral coordination, with 2 elongated C-O distances. Each  $\text{SiO}_6$  octahedron is then corner-connected to 4  $\text{CO}_3$  and 2  $\text{CO}_4$  units. However, for all these stoichiometries, the formation enthalpies are positive. Therefore, and according to the convex hull formalism, the corresponding structures are not metastable.

### 3.3 $\text{SiC}_2\text{O}_6$ : A stable $P2_1/c$ structure

Interestingly enough, only in a wide pressure range between 7.2 and 41 GPa, the  $\text{SiC}_2\text{O}_6$  stoichiometry emerges as thermodynamically stable against the decomposition into the corresponding stable  $\text{SiO}_2$  and  $\text{CO}_2$  polymorphs at those conditions (see Fig. 1). The most stable  $\text{SiC}_2\text{O}_6$  phase is monoclinic, spacegroup  $P2_1/c$  with Si atoms located on  $2a$  sites (0.0,0.0,0.0), C atoms on  $4e$  sites (0.662,0.662,0.755) and three non-equivalent oxygen atoms on  $4e$  sites, at (0.684,0.316,0.287), (0.850,0.052,0.245), and (0.519,0.350,0.735) at 27.5 GPa. The corresponding lattice parameters are  $a=8.492 \text{ \AA}$ ,  $b=4.264 \text{ \AA}$ ,  $c=4.306 \text{ \AA}$ , with  $\gamma=119.992^\circ$ . Given that  $a \approx 2b$ , it can be also described as a  $2 \times 1 \times 1$  supercell of a pseudo-hexagonal phase. The predicted phase consists of almost planar triangular  $\text{CO}_3$  carbonate groups connecting slightly distorted  $\text{SiO}_6$  octahedra through the oxygen atoms.

An electron localization function (ELF) analysis (see Fig. 3) reveals the covalent bond basin associated to the C-O bond (small ring, signature of a double bond) and confirms the partial ionic character of the Si-O bonds (superanionic basin around the oxygen atoms consisting of two lone pairs and a bond basin displaced towards the oxygen atom)<sup>25</sup>. The mixed covalent-ionic character is also clear from the quantum theory of atoms in molecules (QTAIM) charges associated to the Si, C and O atoms, +3.12e, +1.75e and -1.10e, respectively. In contrast to the other structures, it does not present neither edge-sharing of octahedra nor

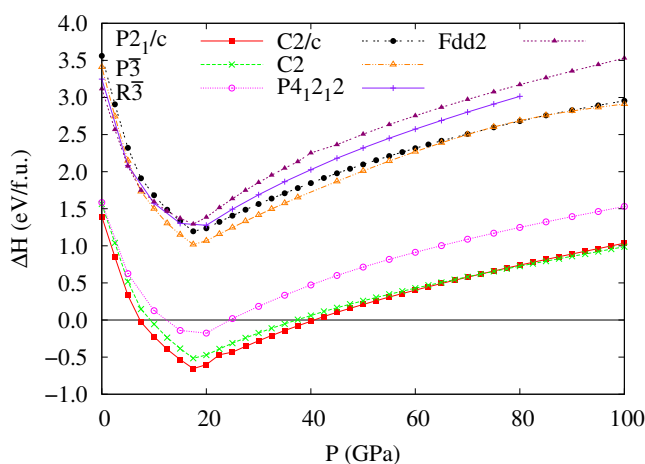


**Fig. 4** Calculated enthalpies of formation as a function of pressure for several structures with  $\text{SiC}_2\text{O}_6$  stoichiometry. The enthalpy of the stable  $\text{SiO}_2$  and  $\text{CO}_2$  polymorphs at the corresponding pressure is taken as the reference enthalpy:  $\Delta H = H(\text{SiC}_2\text{O}_6) - H(\text{SiO}_2) - 2H(\text{CO}_2)$ .

corner-sharing of  $\text{CO}_3$  units. Therefore, it does not violate the 3rd Pauling rule.

### 3.4 $\text{SiC}_2\text{O}_6$ : other proposed structures

In a previous study<sup>11</sup>, we proposed a candidate  $\text{UB}_2\text{O}_6$ -type structure ( $C2/c$ ,  $Z=4$ ) with carbonate units when substituting U and B for Si and C, respectively. After analysing the stability of different  $\text{SiCO}$  configurations generated replacing U and B' for Si, and B for C in the conventional reference structure  $\text{U}_4[\text{B}_n\text{B}'_{8-n}]\text{O}_{24}$  ( $n=1-8$ ), the  $\text{SiC}_2\text{O}_6$  stoichiometry was indeed found to be the most plausible one. However, this potential  $\text{UB}_2\text{O}_6$ -type structure is clearly unstable with respect to the one found after evolutionary searches in the current study.

A detailed analysis of the structural searches performed on the  $\text{SiC}_2\text{O}_6$  stoichiometry (Fig. 4) reveals that whereas all the low enthalpy structures ( $P2_1/c$ ,  $P\bar{3}$ ,  $R\bar{3}$ ) present  $\text{SiO}_6$  octahedra corner-connected through almost-planar  $\text{CO}_3$  units, the  $C2/c$  structure shows  $\text{SiO}_4$  and distorted  $\text{CO}_4$  units after optimization. To further analyze the stability of potential structures with tetrahedral coordination for both, C and Si atoms, we have calculated the enthalpy of structures derived from known tetrahedrally-coordinated polymorphs of  $\text{SiO}_2$  and  $\text{CO}_2$ . In particular, and to reproduce the  $\text{SiC}_2\text{O}_6$  stoichiometry,  $(3 \times 3 \times 1)$ ,  $(1 \times 1 \times 3)$  and  $(\sqrt{2} \times \sqrt{2} \times 1)$  supercells of the  $\alpha$ -cristobalite, tetragonally-distorted  $\beta$ -cristobalite-like and  $\alpha$ -cuarz structures have been generated. Cationic sites have been substituted by Si and C atoms. The resulting space groups of the configurations with the lowest enthalpies for the three derived structures are  $P4_12_12$ ,  $Fdd2$  and  $C2$ , respectively (see Fig. 5).

Interestingly, all the phases derived from the  $\alpha$ -cristobalite,  $\beta$ -cristobalite, and  $\alpha$ -quartz  $\text{Si(C)O}_2$  polymorphs, ( $P4_12_12$ ,  $Fdd2$ ,  $C2$ ) consist of the same tetrahedral structural units than  $C2/c$  and are similar in enthalpy. Also, their formation enthalpy curves versus pressure show a minima region in the same pressure range indicated before. Therefore, there is a favourable pressure range

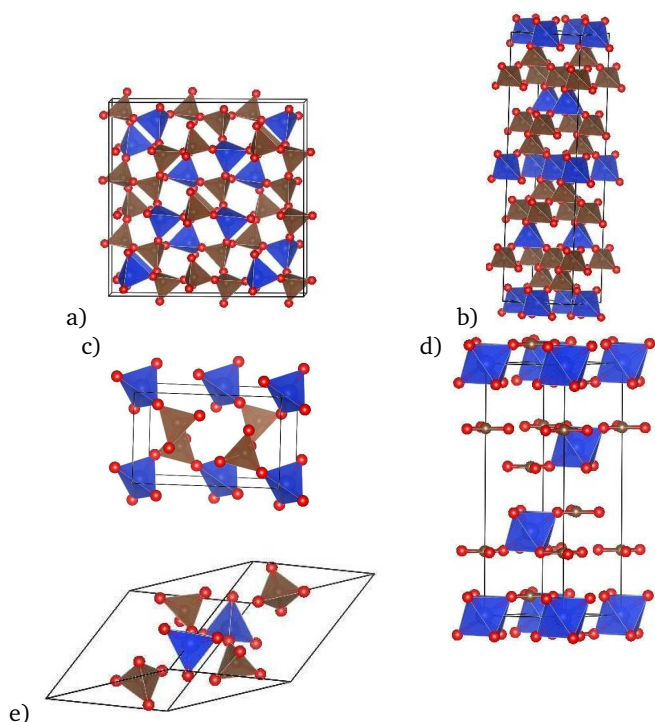


**Fig. 5** Unit cells of the a)  $P4_12_12$ , b)  $Fdd2$ , c)  $C2$ , d)  $R\bar{3}$  and e)  $C2/c$  phases of the  $\text{SiC}_2\text{O}_6$  stoichiometry. Coordination polyhedra for silicon and carbon atoms in blue and brown, respectively.

for their formation. Still, the 4-coordinated phases are 1.67-1.95 eV/ $\text{SiC}_2\text{O}_6$  unit higher in enthalpy than the most stable  $P2_1/c$  phase at the minimum of the enthalpy curves. It implies that the possible temperature-driven stabilization of these phases would require at least 2200 K. It is also in agreement with the recent paper by Santoro *et al* where temperatures higher than 4000 K are needed for the synthesis of a solid solution with an  $\alpha$ -type cristobalite structure<sup>10</sup>. This unstabilization is mainly energetically-related since the energies differ by 1.66-1.99 eV/ $\text{SiC}_2\text{O}_6$  unit at the same pressure (17.5 GPa). Mechanically, all these phases are less compressible than the  $P2_1/c$  phase, in the order  $C2 < C2/c < P4_12_12 < Fdd2$ .

A preference towards the formation of carbonate  $\text{CO}_3$  units is then unveiled. Moreover, the most stable  $P2_1/c$  structure (Fig. 3) resembles the calcite structure found in some carbonates such as  $\text{CaCO}_3$ <sup>26</sup>, with planar  $\text{CO}_3$  units and metals octahedrally coordinated to oxygen atoms. But whereas in the calcite structure each octahedra share corners with other six octahedra, no direct linkage of  $\text{SiO}_6$  octahedra appears in the monoclinic structure, with intercalated  $\text{CO}_3$  units in between. Besides, a pseudo-calcite structure ( $R\bar{3}$ , see Fig. 5d) generated by occupying only 3/4 of the cation sites turns to be unstable with respect to the  $P2_1/c$  structure. Looking at the cationic ( $\text{SiC}_2$ ) framework of the  $P2_1/c$  structure at 27.5 GPa, it can be described as a distorted  $\text{CaCl}_2$ -type structure, with the orthorhombic  $Pnmm$  space group,  $a=7.355 \text{ \AA}$ ,  $b=4.306 \text{ \AA}$ ,  $c=4.264 \text{ \AA}$ , Si atoms on  $2a$  sites (0.0,0.0,0.0) and C atoms on  $4g$  sites (0.338,0.245,0.0), where C atoms form a hcp arrangement, and Si atoms fill octahedral sites in alternated layers.

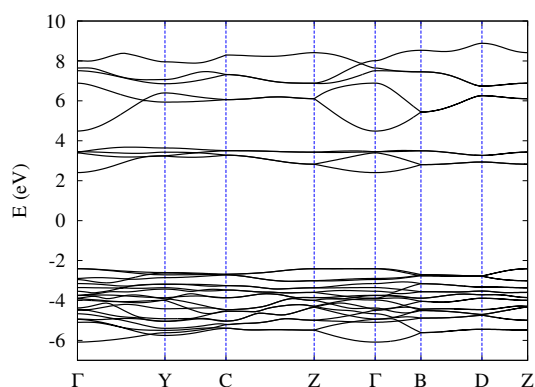


**Fig. 6** Band structure for the  $P2_1/c$  structure at ambient pressure.

### 3.5 Mechanical, electronic and vibrational properties of $P2_1/c$ - $\text{SiC}_2\text{O}_6$

In analogy with the calcite-type compounds, the compressibility of the  $P2_1/c$  structure is clearly anisotropic. This is due to the fact that the C-O bonds are less compressible than the Si-O bonds (the average interatomic C-O and Si-O distances shorten by 1.78 % and 4.11 %, respectively, between room pressure and 50 GPa). Since the  $\text{CO}_3$  units dispose on planes almost perpendicular to the  $c$  axis, the compressibility along this axis is greater ( $\kappa_c=0.053 \text{ GPa}^{-1}$ , being  $\kappa_b=0.002 \text{ GPa}^{-1}$ ). From 0 to 8 GPa, the axis  $a$  is subjected to a negative lineal compressibility, related to the deviation of the  $\text{CO}_3$  units from the plane axial to the  $c$  axis. This modulation disappears when increasing pressure, being the axis  $a$  even less compressible than the  $b$  axis. This pressure-driven tendency to the coplanarity of the  $\text{CO}_3$  units on planes perpendicular to the  $c$  axis is also accompanied by a symmetrization of the  $\text{SiO}_6$  units. A polynomial fitting of the volume-pressure data leads to a bulk modulus of 34.98 GPa ( $B'_0=3.60$ ) at ambient conditions, increasing to 192.43 GPa at 27.5 GPa. The anisotropy also manifests in the elastic constants, with  $C_{22} \approx 2C_{33}$  ( $C_{33}=240.95 \text{ GPa}$  at 27.5 GPa).

It must be also noted that the stishovite structure of  $\text{SiO}_2$  (the one with the lowest enthalpy in the pressure range where the  $\text{SiC}_2\text{O}_6$  structure appears as thermodynamically stable) also shows  $\text{SiO}_6$  polyhedra and, what is more interesting, similar Si-O distances are observed for the  $\text{SiO}_2$  polymorph and the  $\text{SiCO}$  compound at the same pressure.

At ambient conditions, the electronic band structure of the stable  $P2_1/c$  structure (see Fig. 6) shows an insulator character with a high band gap of 4.8 eV, and negligible variation under pressure. Although the highest occupied state appears on the middle of the  $\Gamma$ -Z line, its energy is almost identical at the  $\Gamma$  point. Specifically, the difference between the formally indirect band gap and the direct band gap is of only 2 meV.

The phonon dispersion curves present three well differentiated regions, all with positive frequencies, confirming its dynamical stability (see Fig. 7). The modes with frequencies lower than  $900 \text{ cm}^{-1}$  mainly correspond to bending and Si-O stretching, the modes with frequencies around  $1200 \text{ cm}^{-1}$  can be associated to C-O symmetric stretching modes, and the higher fre-

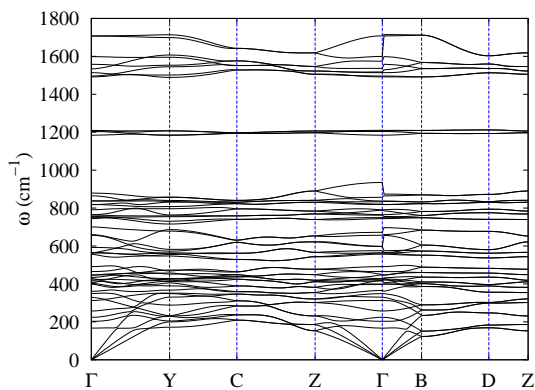


Fig. 7 Phonon dispersion curves for the  $P2_1/c$  structure at 27.5 GPa

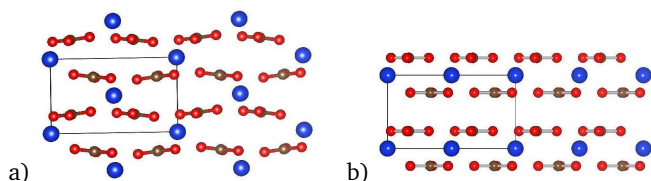


Fig. 8 Crystal structures for the (a)  $P2_1/c$  and (b)  $P\bar{3}$  structures. Larger blue spheres represent Si atoms, smaller brown and red ones correspond to C and O atoms, respectively

quency modes, with frequencies higher than  $1490\text{ cm}^{-1}$  and up to  $1708\text{ cm}^{-1}$  can be assigned to C-O asymmetric stretching modes. The reported experimental infrared spectra of the disordered silicon carbonate phase with  $\text{CO}_3$  units assigned two peaks between  $1500$  and  $1700\text{ cm}^{-1}$  to the C-O antisymmetric stretching<sup>9</sup>. Curiously enough, the calculated infrared frequencies for the C-O antisymmetric stretching range between  $1518$ - $1599\text{ cm}^{-1}$  in good agreement with the experimental data. It must be noted that PBE frequencies tend to be subestimated. It is also interesting to note that in spite of being unstable against decomposition, this phase remains dynamically stable at ambient pressure. It might be then possible to recover it as metastable.

### 3.6 $P\bar{3}$ - $\text{SiC}_2\text{O}_6$ and potential structures at higher pressure

The previously proposed  $P\bar{3}$  structure ( $Z=1$ )<sup>12</sup> appears as thermodynamically stable against decomposition in a slightly smaller pressure range than the  $P2_1/c$  structure, from  $9.4$  to  $37.3\text{ GPa}$  (see Fig. 4). Structurally, both structures are similar as their representation in a common  $P\bar{1}$  subgroup shows (see Fig. 8). The main difference comes from the displacement of the silicon atoms located on the center of the faces to the middle of the edges, going from the  $P2_1/c$  towards the  $P\bar{3}$  structure. It generates a multislabs structure, consisting each slab of two layers of carbonates and a layer of silicon atoms in between. Also, as a consequence of the higher symmetry of the  $P\bar{3}$  structure, the modulation of the  $\text{CO}_3$  units disappears, and the  $\text{SiO}_6$  octahedra has six equal Si-O distances. Then, at  $22.5\text{ GPa}$ , the only Si-O distance is  $1.75\text{ \AA}$ , whereas the Si-O distances for the  $P2_1/c$  structure take three values,  $2 \times 1.74\text{ \AA}$ ,

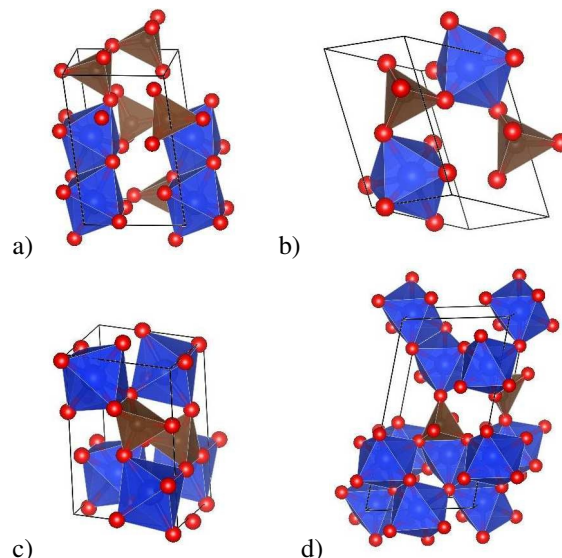


Fig. 9 Unit cells of the lowest enthalpy polymorphs corresponding to the a)  $\text{SiC}_2\text{O}_6$ , b)  $\text{SiCO}_4$ , c)  $\text{Si}_2\text{CO}_6$  and d)  $\text{Si}_3\text{CO}_8$  stoichiometries, at  $100\text{ GPa}$ . Coordination polyhedra for silicon and carbon atoms in blue and brown, respectively.

$2 \times 1.75\text{ \AA}$ , and  $2 \times 1.76\text{ \AA}$ . In analogy with the  $P2_1/c$  structure and since the  $\text{CO}_3$  units dispose in planes perpendicular to the  $c$  axis, the compressibility along the  $c$  axis is considerably higher. What is more, the formation of empty space between the slabs intensifies this effect ( $\kappa_c = 0.09\text{ GPa}^{-1}$ ,  $\kappa_b = 0.0003\text{ GPa}^{-1}$ ), resulting in a lower bulk modulus at ambient conditions of  $10.4\text{ GPa}$ . However, it must not be forgotten that the  $P2_1/c$  structure has the lowest enthalpy in all the thermodynamically stable pressure range. In particular, it is  $166.9\text{ meV/SiC}_2\text{O}_6$  unit lower in enthalpy at  $10\text{ GPa}$ , and although there is a stabilization of the  $P\bar{3}$  structure at higher pressures (the own symmetrization of the  $P2_1/c$  structure signposts it), the  $P2_1/c$  structure is still  $90.13\text{ meV/SiC}_2\text{O}_6$  unit lower in enthalpy at  $35\text{ GPa}$ .

The layered character of the  $P\bar{3}$  structure also suggests the possible influence of van der Waals effects in its stabilization. But, the inclusion of these effects does not alter the relative stability of the phases. For instance, at  $20\text{ GPa}$ ,  $130\text{ meV}$  favors the  $P2_1/c$  structure against the hexagonal structure, reduced to  $120\text{ meV}$  with the inclusion of van der Waals effects. Moreover, the inclusion of the vibrational effects leads to an extra stabilization of the monoclinic structure versus the hexagonal one. In fact, even at  $0\text{ K}$ , slightly lower frequencies for the  $P2_1/c$  structure lead to a zero point energy (phonon contribution to the Helmholtz free energy at  $0\text{ K}$ )  $2.84\text{ meV}$  lower than that of the  $P\bar{3}$  structure. The stabilization is significantly enhanced when temperature, and therefore, entropic contributions are included. For instance, at  $1000\text{ K}$ , the phonon contribution to the Helmholtz free energy is lower by  $26.83\text{ meV}$ .

Finally, at considerable higher pressures (above  $86\text{ GPa}$ ), another structure with tetrahedral  $\text{CO}_4$  units appears to be more favourable energetically (note the change of symbols in Fig. 1 associated to a different structure for the  $\text{SiC}_2\text{O}_6$  stoichiometry and see Fig. 9a)). Therefore, a change of the carbon hybridization



from  $sp^2$  to  $sp^3$  is predicted in close resemblance to the observed in other ionic carbonates<sup>27,28</sup>. The searches performed on the rest of stoichiometries do not reveal any structure stable against decomposition at any pressure. However, in analogy with the  $\text{SiC}_2\text{O}_6$  stoichiometry, there is a preference for the formation of  $\text{CO}_3$  and  $\text{SiO}_6$  units at low pressures and  $\text{CO}_4$  and  $\text{SiO}_6$  units at high pressure (see Fig. 1 and Fig. 9).

## 4 Conclusions

In summary, extensive evolutionary algorithm searches lead to the prediction of the first  $\text{SiCO}$ -based stable crystal structure in a wide pressure range from 7.2 to 41 GPa. The structure of this novel phase with  $\text{SiC}_2\text{O}_6$  stoichiometry and  $P2_1/c$  space group has been fully characterized and proved to be dynamically stable. It is a strongly anisotropic insulator with a wide band gap, consisting of  $\text{SiO}_6$  units corner-connected to  $\text{CO}_3$  units. Crystal structures consisting of tetrahedral  $\text{CO}_4$  and  $\text{SiO}_4$  units are only accessible in this pressure range at temperatures above 2200 K. However, a 4-fold coordination for carbon is predicted at higher pressures for all the stoichiometries. The identification of this new class of stable carbonates at pressures close to the Earth's mantle represents a step forward towards the understanding of the oxide chemistry and opens the way for solving issues in the deep carbon cycle. We hope that our findings will encourage further experimental and theoretical work.

## 5 Acknowledgements

Financial support from the Spanish MINECO CTQ2012-38599-CO2 project and the MALTA-Consolider Ingenio-2010 program under project CSD2007-00045 are gratefully acknowledged. A. M-G also acknowledges a FPI grant from the Spanish MINECO.

## References

- 1 R. M. Hazen and C. M. Schiffrins, *Rev. Mineral. Geochem.*, 2013, **75**, 1–6.
- 2 A. A. Olajire, *J. Pet. Sci. Technol.*, 2013, **109**, 364–392.
- 3 R. M. Hazen, R. T. Downs, A. P. Jones and L. Kah, *Rev. Mineral. Geochem.*, 2013, **75**, 7–46.
- 4 N. Takafuji, K. Fujino, T. Nagai, Y. Seto and D. Hamane, *Phys. Chem. Miner.*, 2006, **33**, 651–654.
- 5 N. H. Sleep and K. Zahnle, *J. Geophys. Res.*, 2001, **106**, 1373–1399.
- 6 J. Wang, L. Zhang, Q. Zeng, G. L. Vignoles, L. Cheng and A. Guette, *Scripta Mater.*, 2010, **62**, 654–657.
- 7 C. R. S. da Silva, J. F. Justo, I. Pereyra and L. V. C. Assali, *Diam. Relat. Mater.*, 2005, **14**, 1142–1145.
- 8 A. Aravindh, A. Arkundato, S. Barman, S. Baroni, B. Bhargava, K. Chandrakumar, W. Chen, R. Cherian, A. D. Corso, S. Datta, S. de Gironcoli, S. S. Dhayal, A. Dixit, S. Dutta, P. D'yachkov, C. Floare, N. Ganguli, S. Ganguly, R. Gebauer, S. Ghosh, P. Giannozzi, G., A. Hatt, K. Hembram, M. Iman, V. Jayalakshmi, C. Jayanthi, T. Kelkar, A. Kumar, J. Lee, M.-S. See, D. Lonappan, P. Mahadevan, S. Mallajosyula, M. Marathe, N. Marzari, B. Melot, N. Miller, J. Morrone, S. Nanavati, A. Nanayakkara, P. Nandi, S. Narashimhan, B. Natarajan, F. Parvin, S. Paul, K. Pradhan, G. Praveena, D. Prasad, H. Poswal, B. Pujari, R. Pushpa, G. Praveena, D. Prasad, H. Poswal, B. Pujari, R. Pushpa, K. Reddy, S. Saha, C. Sbraccia, S. Scandolo, P. Seal, G. Shafai, K. Shanavas, J. Simrall, A. Srirangarajan, V. Srivastava, M. Talati, Y. Tantarungrotechai, K. Tarafder, T. Thomas and T. Uthayathan, *Solid State Commun.*, 2007, **144**, 273–276.
- 9 M. Santoro, F. Gorelli, J. Haines, O. Cambon, C. Levelut and G. Garbarino, *Proc. Natl. Acad. Sci. USA.*, 2011, **108**, 7689–7692.
- 10 M. Santoro, F. A. Gorelli, R. Bini, A. Salamat, G. Garbarino, C. Levelut, O. Cambon and J. Haines, *Nat. Commun.*, 2014, **5**, 3761/1–5.
- 11 A. Morales-García, M. Marqués, J. M. Menéndez, D. Santamaría-Pérez, V. G. Baonza and J. M. Recio, *Theor. Chem. Acc.*, 2013, **132**, 1308/1–5.
- 12 R. Zhou, B. Qu, J. Dai and X. C. Zeng, *Phys. Rev. X*, 2014, **4**, 011030/1–11.
- 13 S. Sen, S. J. Widgeon, A. Navrotsky, G. Mera, A. Tavakoli, E. Ionescu and R. Riedel, *Proc. Natl. Acad. Sci. USA.*, 2013, **110**, 15904–15907.
- 14 A. R. Oganov, R. J. Hemley, R. M. Hazen and A. P. Jones, *Rev. Mineral. Geochem.*, 2013, **75**, 47–77.
- 15 A. R. Oganov and C. W. Glass, *J. Chem. Phys.*, 2006, **124**, 244704/1–15.
- 16 A. R. Oganov, C. W. Glass and S. Ono, *Earth Planet. Sc. Lett.*, 2006, **241**, 95–103.
- 17 A. R. Oganov, S. Ono, Y. Ma, C. W. Glass and A. García, *Earth Planet. Sc. Lett.*, 2008, **273**, 38–47.
- 18 A. Bouibes and A. Zaoui, *Sci. Rep.*, 2014, **4**, 5172.
- 19 G. Kresse and J. Furthmüller, *Phys. Rev. B*, 1996, **54**, 11169–11186.
- 20 J. P. Perdew, K. Burke and M. Ernzerhof, *Phys. Rev. Lett.*, 1996, **77**, 3865–3868.
- 21 G. Kresse and D. Joubert, *Phys. Rev. B*, 1999, **59**, 1758–1775.
- 22 H. J. Monkhorst and J. D. Pack, *Phys. Rev. B*, 1976, **13**, 5188–5192.
- 23 S. Baroni, S. de Gironcoli, A. D. Corso and P. Giannozzi, *Rev. Mod. Phys.*, 2001, **73**, 515–562.
- 24 P. Giannozzi, S. Baroni, N. Bonini, M. Calandra, R. Car, C. Cavazzoni, D. Deresoli, G. L. Chiarotti, M. Cococcioni, I. Dabo, A. D. Corso, S. de Gironcoli, S. Fabris, G. Fratesi, R. Gebauer, U. Gerstmann, C. Gougoussis, A. Kokalj, M. Lazzeri, L. Martin-Samos, N. Marzari, F. Mauri, R. Mazzarello, S. Paolini, A. Pasquarello, L. Paulatto, C. Sbraccia, S. Scandolo, G. Scilauzero, A. P. Seitsonen, A. Smogunov, P. Umari and R. M. Wentzcovitch, *J. Phys.: Condens. Matter*, 2009, **21**, 395502/1–19.
- 25 M. A. Salvadó, P. Pertierra, A. Morales-García, J. M. Menéndez and J. M. Recio, *J. Phys. Chem. C*, 2013, **117**, 8950–8958.
- 26 D. Santamaría-Pérez, O. Gomis, J. A. Sans, H. M. Ortiz, A. Vegas, D. Errandonea, J. Ruiz-Fuertes, D. Martínez-García, B. García-Domene, A. L. J. Pereira, F. J. Manjón, P. Rodríguez-Hernández, A. Muñoz, F. Piccinelli, M. Bettinelli

and C. Popescu, *J. Phys. Chem. C*, 2014, **118**, 4354–4361.  
27 S. Arapan and R. Ahuja, *Phys. Rev. B*, 2010, **82**, 184115/1–8.

28 E. Boulard, D. Pan, G. Galli, Z. Liu and W. L. Mao, *Nat. Comm.*,  
2015, **6**, 6311.